ERHIC INTERACTION REGION DESIGN

C. Montag, B. Parker, V. Ptitsyn, S. Tepikian
BNL, Upton, NY 11973, USA
D. Wang, F. Wang
MIT-Bates, Middleton, MA 01949, USA

This paper presents the current interaction region design status of the ring-ring version of the electron-ion collider eRHIC (release 2.0).

1. Introduction

To study high-energy collisions between polarized electrons and heavy ions or polarized protons, adding a 10 GeV electron accelerator to the RHIC complex is currently being considered. Two approaches for the electron accelerator are studied in parallel: a 10 GeV storage ring with a circumference of 1278 m (one third of the RHIC circumference), and a 10 GeV superconducting energy-recovery linac. Basic machine parameters for the ring-ring version are given in Table I.
The eRHIC interaction region (Figure 2) has to serve different purposes. First of all, both beams have to be focused to obtain small beam sizes at the interaction point (IP), thus maximizing the luminosity. Secondly, the two beams have to be separated to enable focussing as close to the IP as possible. Since beam energies differ by more than an order of magnitude (250 GeV protons vs. 10 GeV electrons), the hadron beam is affected only minimally by electron low-β quadrupoles. Superconducting magnets similar to those used for the HERA luminosity upgrade [1] are foreseen to minimize the detector volume occupied by low-β magnets. These low-β quadrupoles carry an additional dipole coil to provide horizontal beam separation, deflecting the electron beam while leaving the hadron orbit practically unchanged.
The first hadron magnet, Q1, is installed at a distance of 5 m from the IP, requiring sufficient separation between the two beams to guide the electrons through a field-free region outside that hadron quadrupole. Normal-conducting magnetic septum quadrupoles [2] are used to minimize the necessary separation..
The required horizontal beam separation at the 5 m septum is given by the $20\sigma_{e,x}$ beam size of the electron beam, plus the $12\sigma_{p,x}$ size of the hadron beam, plus the thickness of the septum itself. It is therefore necessary to minimize the horizontal size of both beams at the location of the septum. This is accomplished by relaxing the horizontal β function of the hadron beam at the IP somewhat, while simultaneously squeezing the vertical β at the IP to optimize luminosity. This results in an upright beam ellipse at the septum. In the case of the electron beam, the horizontal β function at the septum is minimized by appropriate focussing provided by the low-β quadrupoles.

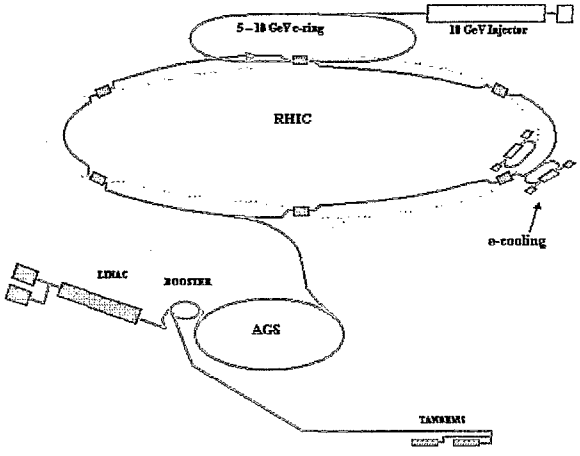

Figure 1: Layout of the planned electron-ion collider eRHIC. Electrons in the electron ring (green) collide with hadrons in the "BLUE" RHIC ring. The "YELLOW" RHIC ring will be equipped with a vertical chicane that provides a separation of 3 m between IP and "YELLOW" ring to accomodate the eRHIC detector.

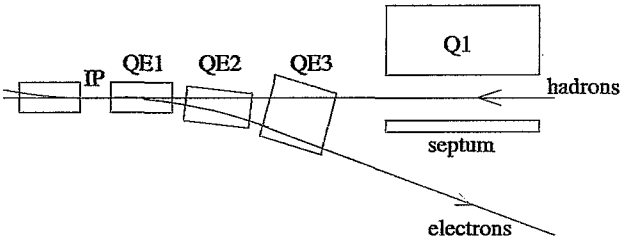

Figure 2: Schematic view of the eRHIC interaction region. The electron low-β triplet (QE1-QE2-QE3) is shared by both beams, but has only negligible effect on the hadron beam. Dipole windings in the superconducting electron triplet quadrupoles provide sufficient separation at the septum of the first hadron quadrupole, Q1, splitting the two beam lines.

Table I Parameter table.

electrons:	
ring circumference [m]	1278
geometric emittance hor./vert. [nm]	50/12.5
β functions hor./vert. [m]	0.19/0.19
particles/bunch	$6.7 \cdot 10^{10}$
number of bunches	120
beam-beam tune shift hor./vert.	0.025/0.05
damping times hor./vert./long. [turns]	1740/1740/870
hadrons:	
ring circumference [m]	3834
geometric emittance hor./vert. [nm]	9/9
β functions hor./vert. [m]	1.04/0.26
particles/bunch	$8.2 \cdot 10^{10}$ (p), $1.0 \cdot 10^{9}$ (Au)
number of bunches	360
beam-beam tune shift hor./vert.	0.005/0.0025
luminosity [$\mathrm{cm}^{-2}\mathrm{sec}^{-1}$]	$2.7 \cdot 10^{32}$

2. Electron IR optics

Since electron β functions at the interaction point are equal, $\beta_x = \beta_y = 0.19\,\mathrm{m}$, focussing is provided by a superconducting quadrupole triplet inside the detector solenoid. Since the horizontal emittance is four times larger than the vertical one, the first and last magnets of that triplet provide focussing in the horizontal plane to keep the horizontal beam size small. The smaller vertical emittance in turn allows for a larger β function in the vertical plane. This occurs inside the second, vertically focussing quadrupole. Figure 3 shows the quadrupole arrangement and β functions, while Table II lists some key parameters of the magnets.

With the first electron quadrupole, QE1, starting at a distance of 1.0 m from the interaction point, this configuration provides a free section of $\pm 1.0\,\mathrm{m}$ around the IP to be used by detector components. The required minimum beam pipe radius is determined by the width of the synchrotron radiation fan that has to be passed safely through these magnets, as well as by the dimensions of the electron beam itself. For the latter, a minimum aperture of $20\sigma_e$ has been used throughout the entire design of the interaction region, thus ensuring sufficient aperture even in the presence of orbit distortions.

Matching into the regular FODO lattice of the arcs can be provided by septum quadrupoles which can be placed anywhere starting at a distance of 10 m from the IP, where the separation between the two beams provides sufficient space for two such magnets, namely one in the electron ring and the other in the hadron ring, to be placed side-by-side.

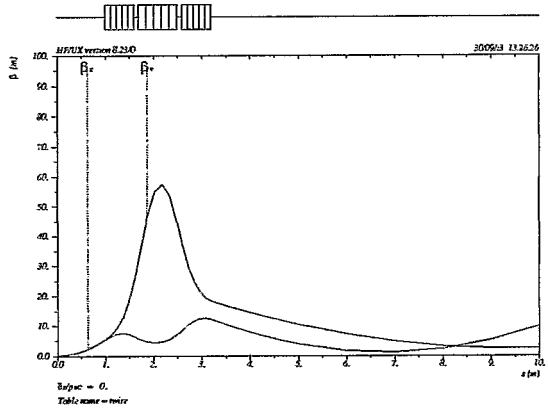

Figure 3: Electron IR lattice of the electron-ion collider eRHIC. Focussing is provided by a superconducting low-β quadrupole triplet (QE1, QE2, QE3).

3. Hadron IR optics

Hadron focussing is provided by a normal-conducting quadrupole doublet, starting 5 m from the IP (Figure 4). Septum quadrupoles are foreseen for both doublet lenses to keep the necessary separation between electron and hadron beams small, thus minimizing the width as well as the power of the resulting synchrotron radiation fan. This also provides the feasibility of placing (septum) quadrupoles in the electron ring where needed, starting at 10 m from the IP. Both lenses are split up into different individual mag-

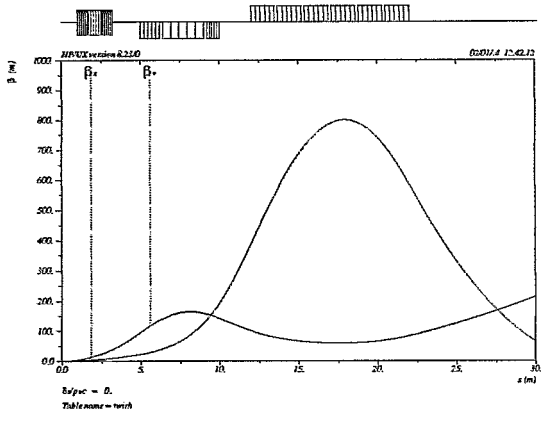

Figure 4: Hadron IR lattice of the electron-ion collider eRHIC. The two lenses of the hadron low-β quadrupole doublet are each split into several individual quadrupoles (Q1, Q1B, and Q1C for the first lens, and Q2, Q2B, Q2C, Q2D, Q2F, and Q2G for the second). The electron low-β quadrupole triplet has only negligible effect on the hadron optics.

Table II Magnet parameters for the electron triplet.

QE1:	
length [m]	0.6
gradient [T/m]	83.3
radius [mm]	24
bending angle left/right [mrad]	2.50/-2.74
shift w.r.t. detector axis left/right [mm]	0/-10
tilt w.r.t. detector axis left/right [mrad]	1.25/-1.37
synchrotron radiation power left/right [kW]	735/882
synchr. rad. power on septum left/right [kW]	466/360
critical photon energy left/right [keV]	9.3/10.1
QE2:	
length [m]	0.8
gradient [T/m]	76.7
radius [mm]	26
bending angle left/right [mrad]	5.30/-2.02
shift w.r.t. detextor axis left/right [mm]	0/-10
tilt w.r.t. detector axis left/right [mrad]	3.90/-2.38
synchrotron radiation power left/right [kW]	2475/360
synchr. rad. power on septum left/right [kW]	0/360
critical photon energy left/right [keV]	14.7/5.6
QE3:	
length [m]	0.6
gradient [T/m]	56.7
radius [mm]	35
bending angle left/right [mrad]	0.0/-4.19
shift w.r.t. detector axis left/right [mm]	0/-10
tilt w.r.t. detector axis left/right [mrad]	3.90/-4.48
synchrotron radiation power left/right [kW]	0/2063
synchr. rad. power on septum left/right [kW]	0/0
critical photon energy left/right [keV]	0/15.5

nets, with pole tip radii tailored according to the varying beam sizes. Pole tip fields are limited to 1.0 T in all magnets to avoid saturation effects at the edges of the magnet poles. Table III lists the main parameters of these magnets.

The most critical situations in terms of aperture and beam size occur at the exits of the first magnets in each lens (Q1 and Q2), as shown in Figures 5 and 6. In the case of the Q1, the $12\sigma_p$ ellipse just fits between the magnet poles, thus leaving no space for the beam pipe if we strictly limit the pole tip field to 1.0 T. This can be remedied by either a slight increase of the pole tip field by a few percent, or, preferably, by shortening this magnet, while simultaneously lengthening Q1B to provide the required overall focussing. The latter will be attempted in the next iteration of the design.

In the second doublet lens, which is horizontally focussing, the beam ellipse is flat. Quadrupole pole tip

Table III Parameter list of the hadron low-β septum quadrupoles

Q1:	
length [m]	1.2
gradient [T/m]	58.3
pole tip radius [mm]	17.2
pole tip field [T]	1.0
Q1B:	
length [m]	2.6
gradient [T/m]	41.7
pole tip radius [mm]	24.0
pole tip field [T]	1.0
Q1C:	
length [m]	0.8
gradient [T/m]	33.3
pole tip radius [mm]	30.0
pole tip field [T]	1.0
Q2:	
length [m]	1.5
gradient [T/m]	20.2
pole tip radius [mm]	49.5
pole tip field [T]	1.0
Q2B:	
length [m]	1.5
gradient [T/m]	17.0
pole tip radius [mm]	58.8
pole tip field [T]	1.0
Q2C:	
length [m]	1.5
gradient [T/m]	16.2
pole tip radius [mm]	61.7
pole tip field [T]	1.0
Q2D:	
length [m]	1.5
gradient [T/m]	16.2
pole tip radius [mm]	61.7
pole tip field [T]	1.0
Q2F:	
length [m]	1.5
gradient [T/m]	16.2
pole tip radius [mm]	61.7
pole tip field [T]	1.0
Q2G:	
length [m]	1.5
gradient [T/m]	17.0
pole tip radius [mm]	58.8
pole tip field [T]	1.0

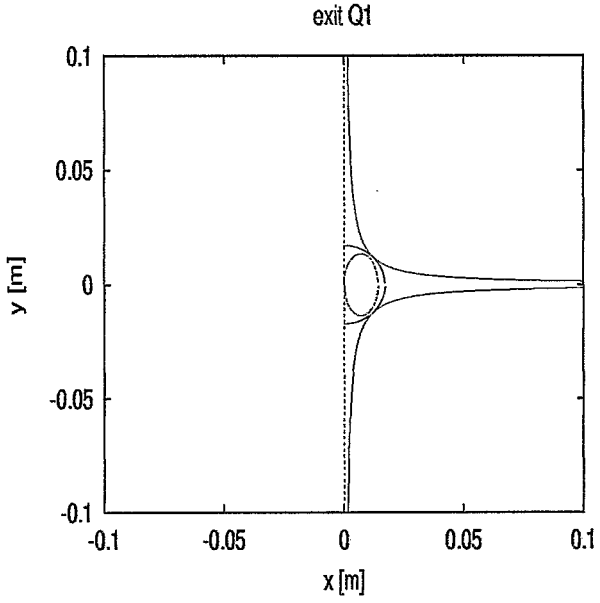

Figure 5: Exit of the Q1 septum quadrupole, with the 12σ beam ellipse and the hyperbolic magnet poles. The semi-circle indicates the pole tip radius.

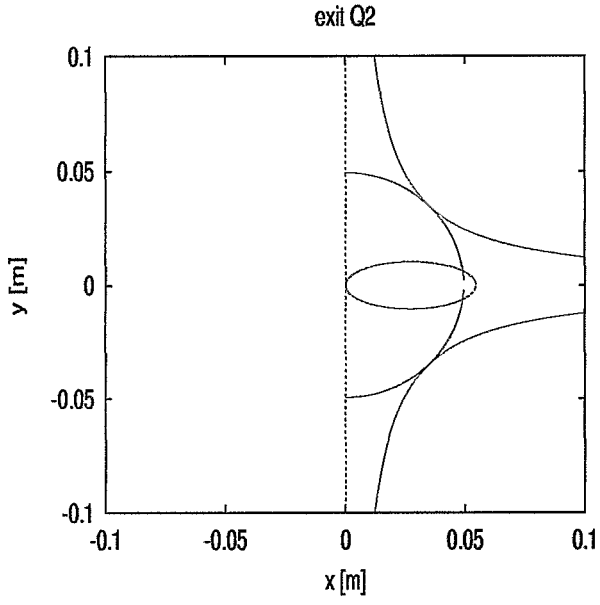

Figure 6: Exit of the Q2 septum quadrupole, with the hyperbolic magnet poles and the 12σ beam ellipse. The semi-circle indicates the pole tip radius.

radii r are chosen such that a small fraction of the $12\sigma_p$ ellipse extends beyond the pole tip radius and between the magnet poles, $2 \cdot 12\sigma_{p,x} > r$. While in all magnets $2 \cdot 12\sigma_{p,x} \leq 1.1 \cdot r$ was achieved, at the exit of the Q2 this is increased to $2 \cdot 12\sigma_{p,x} = 1.15 \cdot r$, see Figure 6. However, since the magnet is set to a pole tip field of 1.0 Tesla, the resulting maximum magnetic field experienced by the $12\sigma_p$ beam is 1.15 Tesla, which is not expected to cause any additional multipoles due to saturation problems.

4. Synchrotron radiation issues

The electron quadrupole triplet inside the detector volume is shared by the hadron beam. The focussing effect on the hadron beam is marginal due to the large energy difference - 10 GeV electrons compared to 250 GeV protons. This large energy difference in turn requires the beams to be separated such that the electrons do not experience the much stronger focussing fields of the hadron low-β quadrupoles. This separation is provided by dipole windings in the superconducting electron low-β quadrupoles. To minimize the necessary beam separation, the first hadron magnet is realized as a septum quadrupole, with a septum thickness of $d_{\text{septum}} = 10\,\text{mm}$, including beam pipes. Since the design apertures for the two beams are $20\sigma_{x,e}$ for the electrons and $12\sigma_{x,p}$ for the hadron beam, the required total separation between the orbits of the two beams at the location of the septum is therefore

$$\Delta x = 12\sigma_{x,p} + 20\sigma_{x,e} + d_{\text{septum}}. \quad (1)$$

Taking into account the β functions shown in Figures 3 and 4, together with the respective emittances according to Table I, the required beam separation is

$$\begin{aligned} \Delta x &= 12 \cdot \sqrt{\beta_{x,p}\epsilon_p} + 20 \cdot \sqrt{\beta_{x,e}\epsilon_e} + d_{\text{septum}} \\ &= 12 \cdot 0.48\,\text{mm} + 20 \cdot 0.45\,\text{mm} + 10\,\text{mm} \\ &= 24.8\,\text{mm}. \end{aligned} \quad (2)$$

When providing this separation using the dipole windings of the superconducting electron low-β quadrupoles, This produces a synchrotron radiation fan that has to be passed safely through the detector beam pipe when providing this separation using the dipole windings of the superconducting electron low-β quadrupoles. Some fraction of this synchrotron radiation fan unavoidably hits the septum on the electron downstream side (right side) of the detector. It was attempted to minimize the power and critical photon energy hitting the septum by distributing the bending angles in the individual dipole coils accordingly.
On the right side, this minimization is accomplished by a soft bend provided by the dipole coils in QE1 and QE2, which produce the part of the synchrotron radiation fan actually hitting the septum. A strong bend in QE3 provides the requried remaining separation angle to achieve sufficient separation at the septum.
This scheme cannot be adopted for the left side since a bend in QE3 there would result in a very wide synchrotron radiation fan further downstream, where it

would require large aperture magnets to pass through. This is not desirable, since large aperture magnets would cover a significant fraction of the detector volume. Instead, a soft bend is provided by the QE1 alone, resulting in a synchrotron radiation fan that is just wide enough to cover the angle between the hadron beam orbit and the inner edge of the septum. The remaining beam separation is then provided by the QE2 dipole coil.

To further minimize the required magnet aperture, all quadrupoles on the right side are shifted towards the inside of the RHIC ring, resulting in an off-center electron orbit through these quadrupoles. The effect of this shift on the electron beam orbit is to be compensated by the dipole coils.

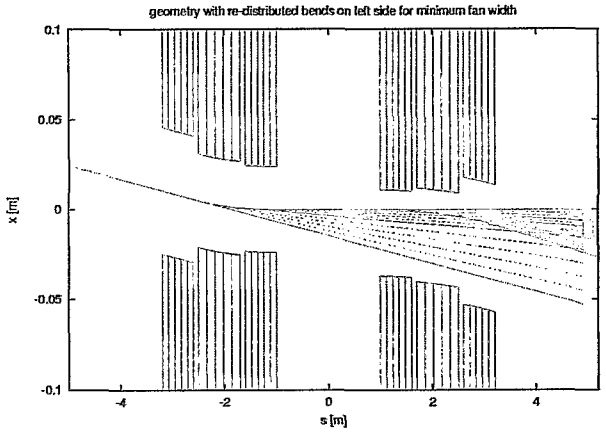

Figure 7: IR geometry and synchrotron radiation fan.

5. Beam-beam simulations

RHIC is currently operating with beams colliding in four of its six interaction points, where beam-beam tune shift parameters of $\xi_x = 0.005$ per IP have been achieved. It is therefore expected to be safe to assume the same beam-beam parameter for the eRHIC hadron IP, especially since it is most likely that by the time eRHIC is operational the number of actual RHIC IPs will be reduced.

The unequal ring circumference for eRHIC might cause additional problems due to the fact that each electron bunch collides with three hadron bunches, thus coupling those bunches to each other [3]. As Figure 8 illustrates, this effect is basically already present in RHIC, where each bunch collides with three other bunches, though in different IPs. To investigate the feasibility of beam-beam interactions with nominal beam-beam tune shift parameters as high as $\xi_x = 0.025, \xi_y = 0.05$ in the eRHIC electron ring, simulation studies have been performed. In these simulations, the accelerator is represented by a linear one-turn matrix. The tunes of this one-turn matrix are

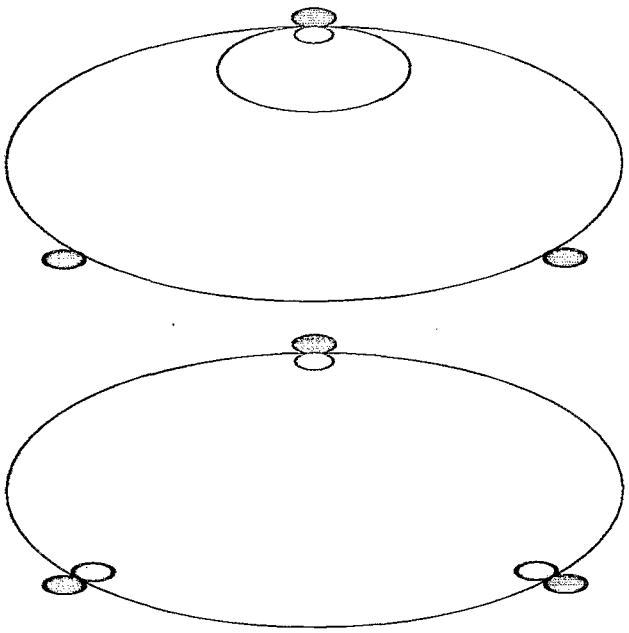

Figure 8: Illustration of one electron bunch (red) interacting with three different hadron bunches (blue) in the eRHIC case (top), and of three bunches in the YELLOW RHIC ring (yellow), each colliding with three different bunches in the BLUE ring (blue) in three interaction points around the RHIC circumference.

scanned in the range below the quarter resonance to determine the best working point. Synchrotron radiation damping and quantum excitation is included, currently based on an older lattice version (release 1.0) that did not produce the emittances required for the interaction region parameters presented here. However, these simulations can nevertheless be considered useful at the present design stage. With a radiation damping time corresponding to 1740 revolutions in the eRHIC electron ring, no beam blow-up and resulting luminosity degradation is observed over a wide tune range around $Q_x = .10$, $Q_y = .15$, as shown in Figure 9. However, the dynamic emittance effect caused by the modification of the $\mathcal{H}$ function,

$$\mathcal{H}(s) = \gamma(s)\eta^2(s) + 2\alpha(s)\eta(s)\eta'(s) + \beta(s)\eta'^2(s), \quad (3)$$

by the presence of a strong beam-beam lens could not be taken into account due to the lack of a consistent lattice solution. Since these effects are mainly observed for tunes very close to the integer or half-integer, this is not expected to significantly alter the results.

Since the nominal hadron bunch intensity had to be lowered by about 20 percent to limit the electron beam-beam tune shift to $\xi_y = 0.05$, we also studied the effect of a larger beam-beam parameter, $\xi_x = 0.031$, $\xi_y = 0.061$, as it results from the regular RHIC bunch intensity of $1.0 \cdot 10^{11}$ protons per bunch. As Figure 10 indicates, there still exist large areas in the working

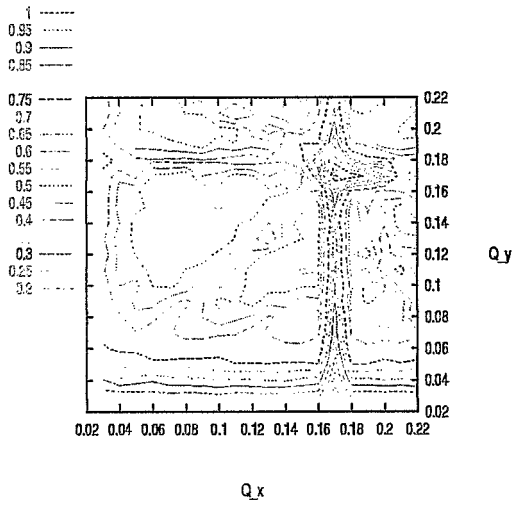

Figure 9: Beam-beam contour plot, $\xi_x = 0.025$, $\xi_y = 0.05$.

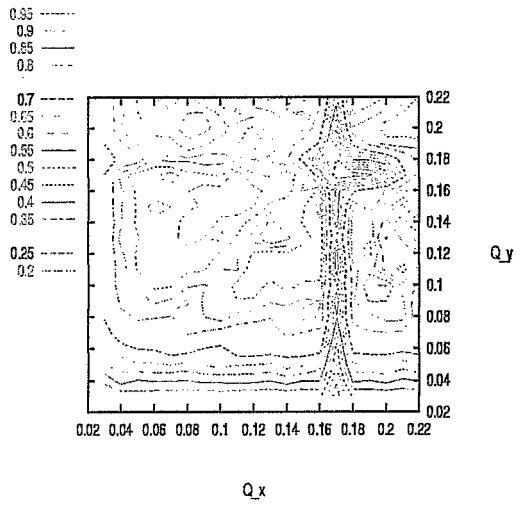

Figure 10: Beam-beam contour plot at full intensity, resulting in a tune shift of $\xi_x = 0.031$, $\xi_y = 0.061$.

diagram where the resulting luminosity is 95 percent of the nominal, geometric value, resulting in a luminosity of $\mathcal{L} = 3.3{\cdot}10^{32}\,\mathrm{cm}^{-2}\mathrm{sec}^{-1}$, an increase of about 20 percent compared to the value given in Table I.

A further increase of the beam-beam tune shift parameter to $\xi_x = 0.035$, $\xi_y = 0.07$ still seems feasible, as Figure 11 indicates. However, the favorable area in

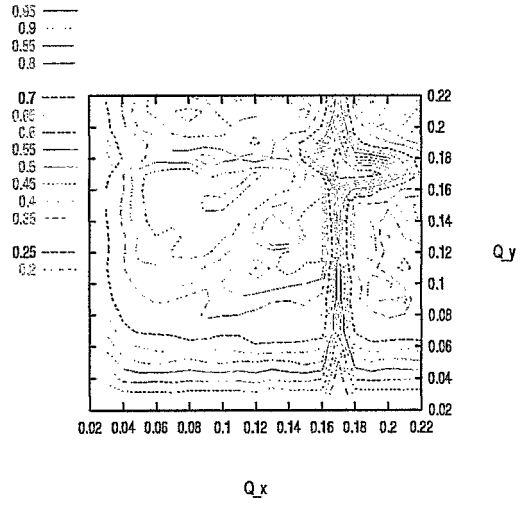

Figure 11: Beam-beam contour plot at increased intensity, leading to beam-beam tuneshift parameters of $\xi_x = 0.035$, $\xi_y = 0.07$.

the tune diagram shrinks to a rather tiny spot around $Q_x = 0.10$, $Q_y = 0.15$. These results still have to be checked by full 6D tracking, including lattice nonlinearities and realistic machine imperfections.

6. Conclusion

An interaction region design for the electron-ion collider eRHIC has been presented that provides a e-p luminosity of $2.7 \cdot 10^{32}\,\mathrm{cm}^{-2}\mathrm{sec}^{-1}$. Beam-beam simulations indicate that this luminosity goal is achievable, and might even be exceeded.

7. Acknowledgements

This work was performed under the auspices of the U.S. Department of Energy.

References

[1] U. Schneekloth (ed.), "The HERA Luminosity Upgrade", DESY HERA 98-05. See also: BNL-68284, BNL-69137, BNL-71432, available at http://www.bnl.gov/magnets/

[2] M. Marx, B. Parker, H. Wuempelmann, "A Concept for a New Type of Magnetic Septum Quadrupole", Proc. EPAC 1996, Sitges, 1996

[3] K. Hirata, E. Keil, "Barycentre motion of beams due to beam-beam interaction in asymmetric ring colliders", Nucl. Instr. Meth. A 292 (1990) 156-168